Stable solvent for solution-based electrical doping of semiconducting polymer films and its application to organic solar cells†

Felipe A. Larrain, [a] Canek Fuentes-Hernandez,[a] Wen-Fang Chou,[a] Victor A. Rodriguez-Toro,[a] Tzu-Yen Huang,[b] Michael F. Toney [b] and Bernard Kippelen *[a]

The immersion of polymeric semiconducting films into a polyoxometalate (PMA) solution was found to lead to electrical doping over a limited depth, enabling the fabrication of organic photovoltaic devices with simplified geometry; yet, the technique was highly solvent selective and the use of nitromethane was found to be limiting. Here, we report on the use of acetonitrile as an alternative solvent to nitromethane. Morphology studies on pristine and PMA doped P3HT films suggest that dopants reside in between the lamella of the polymer, but cause no distortion to the P3HT π–π stacking. With this information, we propose an explanation for the observed solvent-selectivity of the doping method. Degradation studies reveal a superior stability of films doped with PMA in acetonitrile. Based on these findings, we believe that the post-process immersion technique, when dissolving PMA in acetonitrile, is a more suitable candidate to conduct solution-based electrical p-doping of organic semiconductors on an industrial scale.

Broader context

Organic photovoltaics are an emerging thin-film photovoltaic technology that holds promise to deliver flexible, lightweight, low-cost and large-area power harvesting products. While power conversion efficiencies continue to rise beyond 12% in lab-scale devices, efficient charge collection in these cells is typically achieved using interfacial layers with a thickness in the 1–10 nm range, which adds complexity to their fabrication if using most industry-compatible coating techniques. To overcome this problem, our group reported recently single-layer polymer solar cells by combining a solution-based electrical p-doping technique with spontaneous vertical phase separation of amine-containing polymers, leading to a simplified device geometry without sharp heterogeneous interfaces. However, the doping method relied on the use of nitromethane, a solvent unstable in air. In this work, we report on a method using the solvent acetonitrile as an alternative to nitromethane. Not only is the doping solution now stable in air but also cells fabricated using this technique have improved air stability. Furthermore, morphology studies using GIWAXS spectroscopy provide further insight into the doping process. These advances are intended to accelerate the realization of a truly low-cost, large-area PV technology with short energy payback times.

Introduction

Controlled and stable electrical doping of organic semiconductors is desirable for the realization of efficient organic optoelectronic devices. Thus, progress has been made to understand the fundamental doping mechanisms,[1–6] characterize dopant diffusion and doping efficiencies,[7–9] optimize device performance[4,7,10–12] develop efficient molecular n- and p-dopants[13–18] and even explore quantitative dedoping and patterning techniques.[19–22] As a result, from a fabrication perspective, organic semiconductors can be doped today using evaporation methods in a high-vacuum chamber or from solution. Within the solution-based approaches, dopants may be deposited through co-deposition or *via* sequential deposition. In the first approach, dopants are mixed with the semiconductor in a single solution, whereas in the second method, dopants are coated once the organic film is dry, from solvents that do not dissolve the semiconductor. Co-deposition has the advantage that the mixing ratio of dopant to semiconductor is known and can be precisely controlled. However, poor solubility of the dopants in the solvents of the semiconductors and strong interactions between such compounds and the dopants in solution make it challenging to produce doped films with the required morphology for high

[a] *Center for Organic Photonics and Electronics (COPE), School of Electrical and Computer Engineering, Georgia Institute of Technology, Atlanta, GA 30332, USA. E-mail: kippelen@gatech.edu*

[b] *Stanford Synchrotron Radiation Laboratory (SSRL), SLAC National Accelerator Laboratory, Menlo Park, California 94025, USA*

† Electronic supplementary information (ESI) available. See DOI: 10.1039/c8ee00811f

performing organic optoelectronics. Consequently, sequential deposition of dopant molecules is the most suitable alternative to develop large-area devices using high throughput manufacturing.[6] Still, to transform organic semiconductors electrically doped from solution into reliable industrial scale products remains a challenge, in part because current experimental techniques do not comply with the required technical and economic conditions to be conveniently scaled into large area, industrial manufacturing.[23–25]

In 2016, we reported on the use of 12-molybdophosphoric acid hydrate (PMA) to induce p-type doping and crosslinking of neat films of poly[*N*-9′-heptadecanyl-2,7-carbazole-*alt*-5,5-(4′,7′-di-2-thienyl-2′,1′,3′-benzothiadiazole)] (PCDTBT).[26] Later on, a more general approach of sequential solution-based doping was presented, by post-process immersion of donor-like polymer films in PMA-nitromethane solutions. This method renders polymers electrically p-doped over a limited depth of 60 nm and was shown to produce high performing OPV devices, with a power conversion efficiency up to 7.8%, which was comparable to their corresponding reference with an evaporated MoO_3 hole collecting layer.[27] The approach greatly simplified the solar cell geometry and the fabrication complexity as it is vacuum-free and takes place at room temperature. However, critical to the method is the use of nitromethane, a highly unstable solvent, to dissolve PMA. According to the National Fire Protection Association (NFPA), nitromethane is readily capable of detonation, explosive decomposition or explosive reaction at normal temperatures and pressures. While it is known that many solvents readily dissolve PMA, the ability of a PMA solution to electrically dope an organic semiconductor film is highly dependent on the selected solvent. Thus, as long as the post-process immersion technique relies on the use of nitromethane, its applicability to large-scale fabrication of organic solar cells would be limited.

Here, we report on the use of acetonitrile, an air-stable solvent, as an alternative to nitromethane to enable PMA-based electrical doping of organic semiconductors within a limited depth from the surface. The morphology of doped organic films (using PMA dissolved in nitromethane or acetonitrile) was studied using grazing-incidence wide-angle X-ray scattering (GIWAXS) and the data revealed that the dopant molecules intercalate between the P3HT lamella but cause no change in the π–π stacking. Based on these findings, we propose an explanation for the observed solvent-selectivity of the PMA doping method. Finally, we validated the use of acetonitrile to fabricate OPVs and discovered that these devices showed increased stability when exposed to normal atmospheric conditions, compared to reference devices fabricated using nitromethane.

Results and discussion

The solvent-screening process began by looking into chemicals that would dissolve the polyoxometalate at room temperature, would not distort the morphology of the organic film when used in sequential solution-based doping, and would be stable in air at room temperature and 1 atmosphere according to the NFPA 704 standard. The search was limited to chemicals with a stability rating of 2 or less, that is, solvents that may undergo violent chemical change at elevated temperatures and pressures, but are not readily capable of detonation at normal temperatures and pressures. The search was further constrained by selecting only polar solvents, in hindsight of our previous findings using nitromethane and ethanol, both polar solvents. Finally, chemicals were ranked according to their distance to nitromethane in the Hansen space, and chosen with a distance to nitromethane that is equal or below 16.64 (which is the distance between ethanol and nitromethane according to their Hansen solubility parameters) (Table S1, ESI†).

Hence, the following solvents were chosen: 2-propanol, 2-methoxyethanol, dimethyl sulfoxide, dimethylformamide and acetonitrile. PMA was dissolved using each solvent, and P3HT films were immersed at room temperature in these different solutions. Then, the transmittance spectrum of these films was compared against that of a pristine film with the same thickness. Although all selected solvents readily dissolved PMA, only one produced a solution that significantly altered the transmittance of efficient electrical doping (Fig. S1, ESI†). That solvent is acetonitrile, anhydrous, 99.8% purity, purchased from Sigma Aldrich and used as received in inert atmosphere.

The optical properties of P3HT films immersed for 30 min in a 0.5 M solution of PMA in acetonitrile (PMA-im-P3HT) were studied by comparing their transmittance spectra against those of pristine P3HT and P3HT immersed similarly in a 0.5 M solution of PMA in nitromethane (Fig. 1). The normalized change of transmittance $\Delta T\ T^{-1}$ as a function of wavelength (inset of Fig. 1b) reveals the same spectral signatures reported for PMA-im-P3HT films when PMA was dissolved in nitromethane. That is, changes in the region where $\Delta T\ T^{-1} < 0$ correlate with the P3HT polaron bands, and deviations in the region where $\Delta T\ T^{-1} > 0$ correlate to the bleaching of the main π–π* absorption bands.[28,29] The data suggest electrical p-doping into the depth of the organic film. But, additional electrical and physical characterization of the surface and bulk of the doped semiconductor is required to determine if the doping is as effective as when using PMA in nitromethane or less, as we found and reported in the past using PMA dissolved in ethanol.[27]

Thus, the surface properties of PMA-im-P3HT films were studied using a Kelvin probe inside a nitrogen-filled glovebox. The results show a work function (WF) change from 4.4 eV in pristine P3HT to 4.8 eV in PMA-im-P3HT, whether nitromethane or acetonitrile is used to dissolve the polyoxometalate. The change was observed after only 10 s of immersion, and it remains constant for longer immersion times (1 min or 10 min as illustrated in Fig. 1c). This confirms that the p-type electrical doping effect saturates, just as reported earlier.[27] Such a variation in Fermi level energy, when neglecting the presence of surface dipoles, also indicates a change in carrier density of about 10^6 cm^{-3}, if measured at room temperature. This is important because, if electrical p-doping is indeed the cause, then the

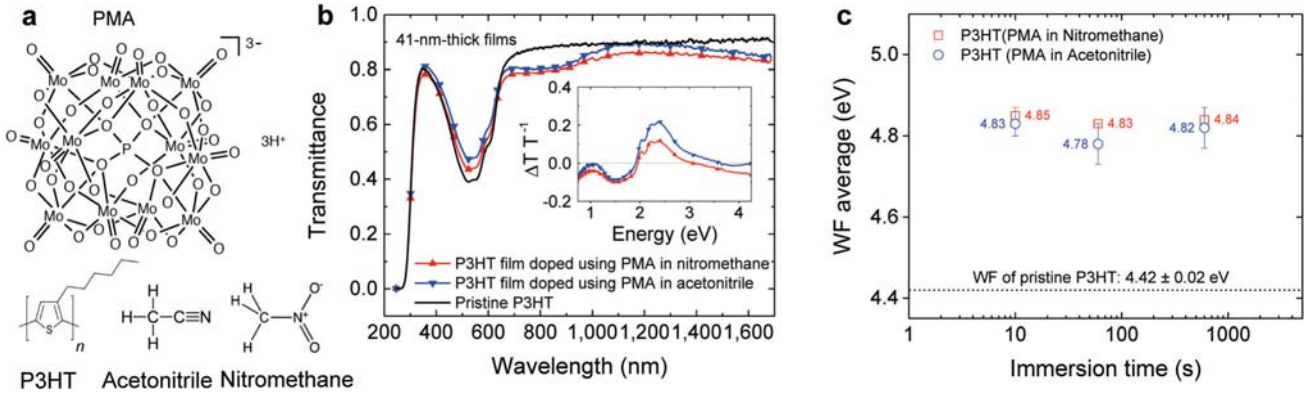

Fig. 1 Optical and electrical properties of P3HT films immersed in a PMA solution in acetonitrile or nitromethane. (a) Chemical structures of phosphomolybdic acid (PMA), nitromethane, acetonitrile and poly(3-hexylthiophene-2,5-diyl) (P3HT). (b) The transmittance of 41 nm-thick pristine P3HT and PMA-im-P3HT (after post-process immersion for 30 min in 0.5 M PMA solution in either nitromethane or acetonitrile) films, with the normalized change in the transmittance data in the inset. (c) WF values of 188-nm thick PMA-im-P3HT layers immersed in 0.5 M solution of PMA in nitromethane or acetonitrile for varying immersion times. Error bars represent statistical variations over a minimum of four spots on each film.

carrier density variation should correlate with a conductivity increase of up to 6 orders of magnitude, starting in the μS cm^{-1} region for pristine P3HT and reaching values in the S cm^{-1} region for doped P3HT.

To confirm this claim, the doping profile, overall penetration depth of dopants and conductivity of PMA-im-P3HT films were investigated for PMA in acetonitrile. In our previous work, the reduction of molybdenum in PMA/PTA-im-P3HT films alongside the oxidation of sulfur from P3HT demonstrated oxidative doping to a limited depth. As a consequence, the focus now was on the characterization of the molybdenum profile into the bulk of the organic layer, obtained by conducting depth profile measurements of PMA-im-P3HT films using a time-of-flight secondary ion mass spectrometry system (IONTOF ToF SIMS). All P3HT layers were coated onto ITO/glass substrates for ease of data processing. Accordingly, depth profiles of molybdenum (attributed to PMA), carbon (attributed to P3HT) and indium (attributed to ITO) cations were measured in PMA-im-P3HT films when PMA was dissolved in nitromethane (Fig. 2a) or acetonitrile (Fig. 2b). The comparison of such profiles (Fig. 2c) shows that the distribution of molybdenum cations has an exponential shape in both cases, and has a decay constant of 15–20 nm when using PMA in nitromethane and 20–25 nm when dissolving PMA in acetonitrile. Indeed, the density of dopants is below 4% of its peak at *ca.* 60 nm from the surface of the film, using either nitromethane or acetonitrile. With these data, the conductivity of a 188 nm-thick PMA-im-P3HT film was estimated, after immersion in a PMA solution in acetonitrile for 1 min. A sheet resistance of 40.9 ± 1.0 kΩ sq^{-1} was found using the four point probe method, which translates into a conductivity of 4.1 S cm^{-1} when assuming 60 nm of the bulk is electrically p-doped. This value is in good agreement with previously reported conductivity data, and is consistent with the WF variation measured using the Kelvin probe.

In order to elucidate why the doping capability of the PMA solution is solvent dependent, the morphology of PMA doped films was investigated when the polyoxometalate is dissolved in various solvents. In addition to acetonitrile, nitromethane and

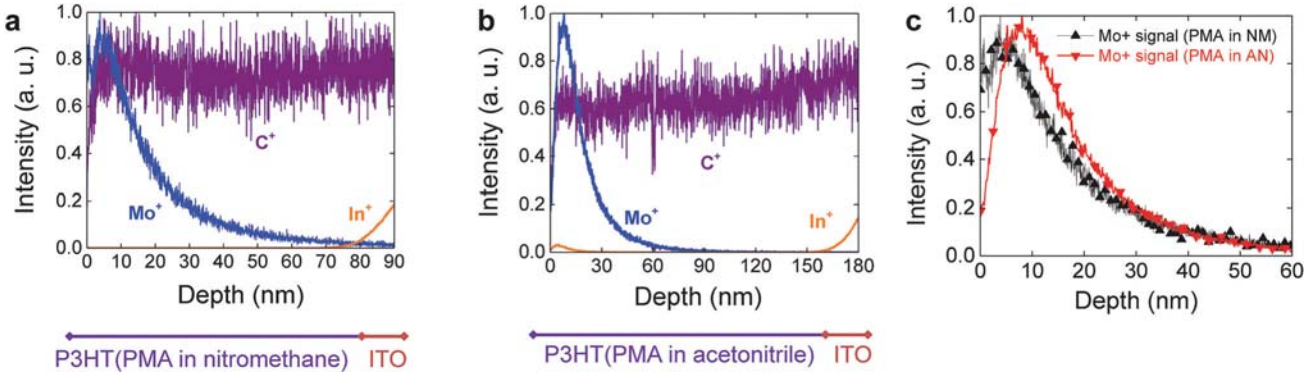

Fig. 2 Vertical profile of P3HT films measured using mass spectrometry. (a) Normalized signals for Mo+, C+ and In+ cations as they are measured into the depth of a P3HT film immersed for 1 min in PMA in nitromethane. (b) Normalized signals for Mo+, C+ and In+ cations as they are measured into the depth of a P3HT film immersed for 1 min in PMA in acetonitrile. (c) Direct comparison of normalized signals for Mo+ cations as they are measured into the depth of a P3HT film immersed for 1 min in PMA in nitromethane (black arrows), and into the depth of a P3HT film immersed for 1 min in PMA in acetonitrile (red arrows).

ethanol were chosen, as the latter two produce a PMA solution capable of doping, but PMA-nitromethane is significantly more effective than PMA-ethanol to dope organic films. As a consequence, the direct comparison is correlated back to the dissimilar effectiveness of these doping solutions, as reported in the past.[27]

Therefore, acetonitrile, nitromethane and ethanol were used to dissolve the polyoxometalate and the morphology of PMA-im-P3HT films fabricated on Si substrates was analyzed using GIWAXS (Fig. 3). As expected, the images show that the preferred orientation of P3HT on the SiO_2 surface is edge-on, with distinctive (100), (200) and (300) lamellar peaks observed in the out of plane direction with q values of 0.37 $Å^{-1}$, 0.77 $Å^{-1}$ and 1.14 $Å^{-1}$ (Fig. 3b). Also as expected, there is a clear peak in the (010) direction with a q value of 1.68 $Å^{-1}$ in the in-plane line profile (d spacing *ca.* 0.37 nm), which is due to the π–π stacking of P3HT.

Interestingly, the PMA doping does not appear to alter the location of the peaks in the in-plane line profile, which implies no change of the π–π stacking distance of P3HT. Instead, additional peaks appear in the out-of-plane line profile of P3HT samples doped with PMA, when the polyoxometalate is dissolved in either nitromethane or acetonitrile, pointing to the intercalation of doping molecules between P3HT lamella. Specifically, in doped samples using PMA in nitromethane or acetonitrile, near the (200) diffraction, the original neat P3HT peak at 0.77 $Å^{-1}$ of the out-of-plane line profile appears next to a new peak at 0.69 $Å^{-1}$. Moreover, near the (300) diffraction, there is a new peak at 1.03 $Å^{-1}$, in addition to the original peak at 1.14 $Å^{-1}$. Thus, the GIWAXS data show that the dopant molecules, when using PMA dissolved in nitromethane or acetonitrile, become intercalated between the lamellar while producing no distortion in the π–π stacking of P3HT. The lamella d-spacing expands from 16.53 Å in pristine P3HT (consistent with the literature[30]) to 18.21 Å in the doped P3HT or by nearly 1.68 Å. However, such an effect is not present when immersing P3HT films into PMA in ethanol. This is consistent with the less effective doping of the PMA-ethanol solution as observed in the past.

As reported in 2017, electrical p-doping using a solution of PMA in nitromethane may be used to fine tune the electrical properties of the photoactive layer of an OPV, producing embedded hole-collecting interlayers through a simple film immersion process.[27] Consequently, the performance of OPVs immersed in a 0.5 M solution of PMA in nitromethane or acetonitrile for 1 min was investigated. All OPV devices were fabricated with a 200 nm-thick PMA-im-P3HT:ICBA photoactive layer, on top of an ITO/polyethylenimine ethoxylated (PEIE) electron-collecting bottom electrode, and with a Ag top electrode.

The data show that the performance of PMA-doped OPV devices using PMA in acetonitrile is comparable to that of OPVs made using PMA in nitromethane or MoO_3, under simulated AM 1.5G solar illumination (Fig. 4, Table 1 and Fig. S2, ESI†). Moreover, OPV devices that were immersed for longer times show comparable photovoltaic performance to those immersed for one min only, confirming that the effect saturates. Overall, these data validate the use of acetonitrile to fabricate OPVs with photovoltaic performance comparable to that of solar cells doped using PMA in nitromethane. However, longer OPV immersion time may be undesirable, as J–V characteristics of OPV devices immersed for 10 min and 30 min show an increase in their leakage current under reverse bias, when measured in the dark (Fig. S3, ESI†). These effects have been correlated in the past with a decreased parasitic shunt resistance, which is detrimental to the device performance under light intensities below 1 sun illumination.[31,32]

All unencapsulated OPV devices were further studied by measuring their photovoltaic performance after exposing them to air, in dark conditions. The results show that OPV devices doped using PMA, whether dissolved in nitromethane or acetonitrile, exhibit an s-shape in the fourth quadrant of their J–V characteristics. Interestingly, all s-shapes are eliminated after

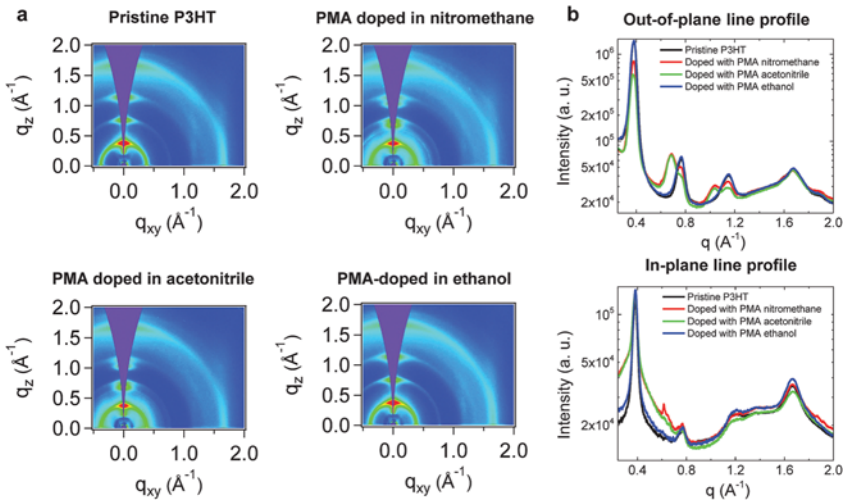

Fig. 3 GIWAXS data as measured on pristine and PMA doped P3HT, when using various solvents to dissolve the PMA. (a) Two-dimensional GIWAXS data converted to q-space for pristine P3HT and P3HT immersed in PMA solutions in nitromethane, acetonitrile or ethanol for 60 s. (b) One-dimensional scattering profiles (out-of-plane and in-plane profiles), obtained from the two-dimensional GIWAXS data.

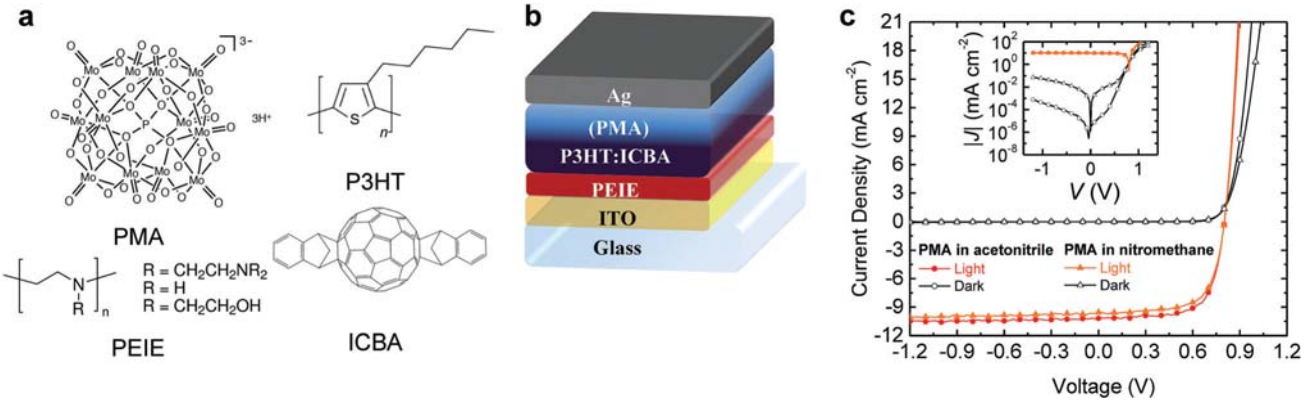

Fig. 4 OPV devices doped with PMA in acetonitrile or nitromethane, measured in the dark and under 1 sun illumination. (a) Chemical structures of phosphomolybdic acid (PMA), poly(3-hexylthiophene-2,5-diyl) (P3HT), indene C_{60} bisadduct (ICBA) and polyethylenimine 80% ethoxylated (PEIE). (b) Structure of OPVs doped with PMA. (c) Direct comparison of *J*–*V* characteristics measured in the dark and under 1 sun illumination.

Table 1 OPV device performance. Photovoltaic performance parameters measured under simulated 100 mW cm^{-2} AM 1.5G illumination. The data represent average values and standard deviations measured over a total of 24 samples

Structure (comments)	J_{SC} (mA cm^{-2})	V_{OC} (mV)	FF	PCE (%)	Number of devices
ITO/PEIE/P3HT:ICBA (200 nm)/MoO_3/Ag (reference)	9.3 ± 0.2	788 ± 6	71 ± 0	5.2 ± 0.1	5
ITO/PEIE/PMA-im-P3HT:ICBA (200 nm)/Ag (PMA dissolved in nitromethane, 1 min immersion)	9.3 ± 0.4	804 ± 1	66 ± 1	4.9 ± 0.2	5
ITO/PEIE/PMA-im-P3HT:ICBA (200 nm)/Ag (PMA dissolved in acetonitrile, 1 min immersion)	9.9 ± 0.3	802 ± 5	68 ± 1	5.4 ± 0.2	5
ITO/PEIE/PMA-im-P3HT:ICBA (200 nm)/Ag (PMA dissolved in acetonitrile, 10 min immersion)	9.5 ± 0.4	810 ± 3	71 ± 1	5.4 ± 0.2	5
ITO/PEIE/PMA-im-P3HT:ICBA (200 nm)/Ag (PMA dissolved in acetonitrile, 30 min immersion)	9.0 ± 0.5	808 ± 4	70 ± 1	5.1 ± 0.3	4

10 min of light soaking under simulated AM 1.5G solar illumination. In other words, the exposure to simulated sunlight corrects the observed s-shape. As reported previously,[33] s-shapes observed in *J*–*V* characteristics of OPVs may be attributed to reversible changes of the work function value of indium-tin-oxide (ITO) under prolonged exposure to ultraviolet light in inert atmosphere, or air. Thus, we speculate that these s-shapes are caused by the adsorption of oxygen on the PEIE-treated ITO bottom contact, when OPV devices are exposed to air. This is consistent with the removal of such s-shapes following light soaking with the solar simulator, as the UV irradiation produces desorption of oxygen from the ITO in inert atmosphere.

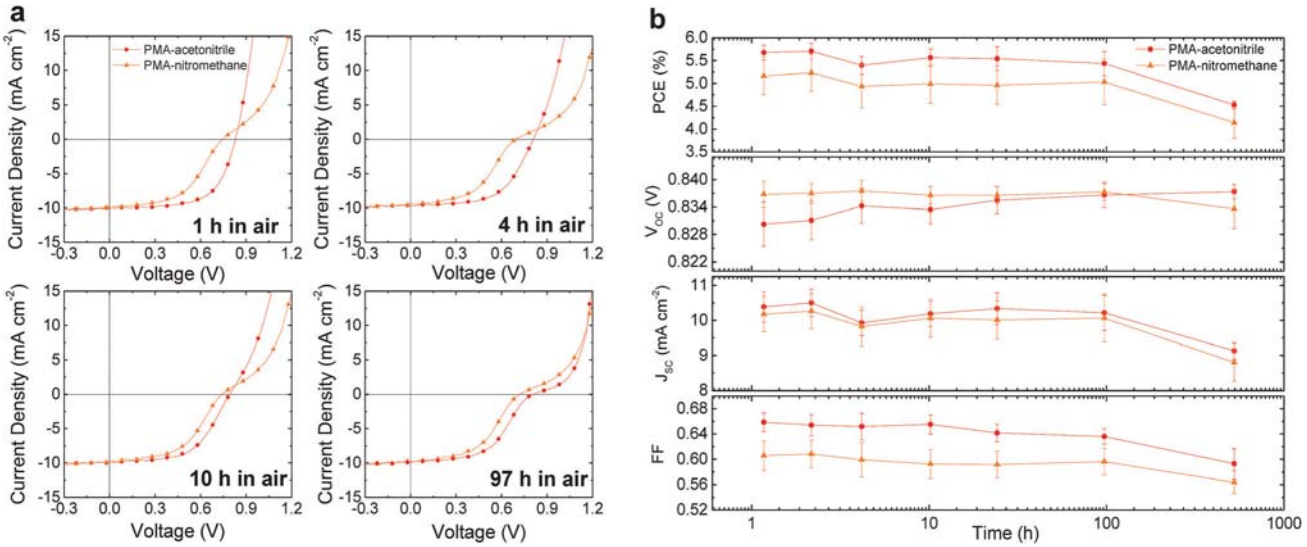

Fig. 5 Air stability of OPV devices doped with PMA in acetonitrile or nitromethane. (a) Direct comparison of the *J*–*V* characteristics of comparable 200 nm-thick PMA-im-P3HT:ICBA OPVs, doped using PMA in acetonitrile or PMA in nitromethane, and exposed to air for up to 97 h. (b) Temporal evolution of photovoltaic parameters for 200 nm-thick PMA-im-P3HT:ICBA OPVs exposed to air at room temperature and in the dark for up to 524 h. All measurements were conducted after 10 min soaking under 1 sun illumination in a N_2-filled glovebox.

Furthermore, if the light soaking mechanism is used before each measurement, OPVs made using PMA in nitromethane or acetonitrile remain stable for up to 524 h in air (Fig. 5), retaining 80% of their initial PCE.

It is worth noting that the appearance of the s-shape in the *J–V* characteristics of OPVs doped with PMA in acetonitrile is delayed, when compared to OPVs made using PMA in nitromethane (Fig. 5a). The difference is noticeable up to 10 h of air exposure, and seems negligible after 97 h of air exposure in all devices (Fig. S4, ESI†). Hence, OPV devices made using PMA dissolved in acetonitrile show increased air stability compared to similar devices fabricated using PMA dissolved in nitromethane. Finally, it is also important to note that OPV devices made using an evaporated 10 nm-thick MoO_3 layer exhibit s-shapes in the fourth quadrant of their *J–V* characteristics as well, but such a feature takes longer air exposure to appear. Although there are slight signs of degradation after 4 h of air exposure, s-shapes comparable to those found in PMA-doped OPV devices degraded in air for 97 h appear after 524 h of similar air exposure (Fig. S5, ESI†).

Conclusions

An alternative, stable solvent to dissolve PMA that also enables electrical doping of organic semiconductors within a limited depth from the surface is reported. Results show that the use of nitromethane as the solvent of PMA is not critical to enable electrical p-doping of semiconducting films. Instead, acetonitrile, when used to dissolve the polyoxometalate, produces organic films with comparable optical, electrical and physical properties to those immersed in PMA in nitromethane.

Based on the morphological analysis of PMA-im-P3HT films using GIWAXS, the solvent (either nitromethane or acetonitrile), in addition to dissolving the polyoxometalate, is found to play a critical role in facilitating the intercalation of dopants into the P3HT in between the lamella. That is, the PMA doping technique is solvent-selective as it requires not only a solvent that dissolves PMA, but also that facilitates the placement of dopants in between the polymer lamella, physically enabling electrical p-doping to take place. Conversely, the weaker optical and electrical signatures of doping observed in PMA-im-P3HT films when using ethanol to dissolve PMA[27] are consistent with the physical lack of dopants in between the lamellar stacking of P3HT. At best, the effects reported in the past correspond to doping along the surface of the film. Both the data and proposed explanation are offered as a step forward in elucidating the doping mechanism.

Finally, OPV devices made using PMA dissolved in acetonitrile showed increased stability (or delayed appearance of an s-shape in the fourth quadrant of the *J–V* characteristics under 1 sun illumination) when exposed to atmospheric conditions, compared to reference devices fabricated using PMA in nitromethane. Based on these findings, the post-process immersion technique, when dissolving PMA in acetonitrile, is found to be a more suitable candidate to conduct solution-based electrical p-doping of organic semiconductors at industrial scale.

Future research will focus on further testing the robustness of this technique by elucidating the cause behind the accelerated but seemingly reversible degradation that takes place on doped OPVs exposed to air, and investigating if it can be prevented.

Experimental

PMA doping of P3HT using PMA dissolved in acetonitrile or nitromethane

ITO-coated soda lime float glass sheets (Colorado Concept Coatings LLC) with a sheet resistance of 9–15 Ω sq^{-1} and VWR glass Micro Slides #48300-025 were cleaved into 1″ by 1″ pieces and used as substrates for P3HT semiconducting films. The substrates were solvent cleaned in sequential ultrasonic baths of Liquinox detergent in distilled water, distilled water, acetone and 2-propanol, each lasting 40 min and at a temperature of 40 °C, and blown dry with N_2. Then, the substrates were transferred into a N_2-filled glove box.

Poly(3-hexylthiophene) (P3HT, 4002-E, Rieke Metals, lot# BS19-90) was weighed on an electronic scale in air and added to two amber glass vials, each with a magnetic stirrer. The vials were transferred to a N_2-filled glove box for further processing. In the first vial, the P3HT was dissolved to a concentration of 10 mg ml^{-1} using chlorobenzene. In the second vial, the P3HT was dissolved to a concentration of 30 mg ml^{-1} using 1,2-dichlorobenzene. Both solutions were magnetically stirred overnight at 500 rpm at room temperature.

The 10 mg ml^{-1} solution of P3HT in chlorobenzene was filtered using a 0.2 μm-pore PTFE filter and spun coated onto the VWR glass slides at 800 rpm, 10 000 rpm s^{-1} for 30 s, dispensing 200 μl of solution per sample. Then, samples were left in glass petri dishes to solvent anneal for 1 h and thermally annealed on a hot plate at 150 °C for 10 min.

The 30 mg ml^{-1} solution of P3HT in 1,2-dichlorobenzene was filtered using a 0.2 μm-pore PTFE filter and spun coated onto the ITO-coated glass slides at 800 rpm, 10 000 rpm s^{-1} for 30 s, dispensing 200 μl of solution per sample. Then, samples were left inside glass petri dishes to solvent anneal for 3 h and thermally annealed by placing them on a hot plate at 150 °C for 10 min.

The as-made P3HT films processed from chlorobenzene were dipped into a 0.5 M solution of 12-molybdophosphoric acid hydrate (PMA, Alfa Aesar, M_w = 1825.25 g mol^{-1}, lot #M29C036) in nitromethane or acetonitrile for 30 min and then thoroughly rinsed with pure solvent, to remove PMA residues from their surface. The as-made P3HT films processed from 1,2-dichlorobenzene were similarly dipped into a 0.5 M PMA solution in nitromethane or acetonitrile for 1 min, 10 min or 30 min and rinsed using pure solvent.

The work function or Fermi level of the P3HT films processed from 1,2-dichlorobenzene was measured using a Kelvin probe located inside a N_2-filled glove box. The samples were transferred in between glove boxes in a sealed container filled with N_2. The work function of each film was measured at 4 different spots on the substrate and adjusted by measuring

the work function of freshly peeled highly ordered pyrolytic graphite (HOPG) with a known work function of 4.6 eV.

Variable angle spectroscopic ellipsometry (J. A. Woollam Co.) was used to measure the UV-vis-NIR transmission spectrum of P3HT films processed from chlorobenzene.

The depth profile of PMA-doped P3HT films was characterized using a time-of-flight secondary ion mass spectrometry system (IONTOF ToF SIMS), to characterize the molybdenum profile. The system was operated using a surface charge stabilizing beam (flood gun), a bismuth ion beam to detect the ions at the surface of the film and an oxygen ion beam to drill into the film. The depth of the crater was measured using a profilometer in air (Dektak 6M Stylus Profiler, Veeco, Plainview, NY), and the obtained value was used to scale the depth profile data.

GIWAXS analysis of P3HT films immersed into PMA in ethanol, nitromethane or acetonitrile

Silicon wafers (University Wafers, part# S4N01SP) were cleaved into 1″ by 1″ pieces and used as substrates for P3HT semiconducting films. The substrates were solvent cleaned in sequential ultrasonic baths of Liquinox detergent in distilled water, distilled water, acetone and 2-propanol, each lasting 40 min and at a temperature of 40 °C, and blown dry with N_2. Then, the substrates were transferred into a N_2-filled glove box.

Poly(3-hexylthiophene) (P3HT, 4002-E, Rieke Metals, lot# BS19-90) was weighed on an electronic scale in air and added to an amber glass vial with a magnetic stirrer. The vial was transferred to a N_2-filled glove box where the P3HT was dissolved to a concentration of 10 mg ml^{-1} using chlorobenzene. The solution was magnetically stirred overnight at 500 rpm at room temperature.

The 10 mg ml^{-1} solution of P3HT in chlorobenzene was filtered using a 0.2 μm-pore PTFE filter and spun coated onto the VWR glass slides at 800 rpm, 10 000 rpm s^{-1} for 30 s, dispensing 200 μl of solution per sample. Then, samples were left in glass petri dishes to solvent anneal for 1 h and thermally annealed on a hot plate at 150 °C for 10 min.

The as-made P3HT films processed from chlorobenzene were dipped into a 0.5 M solution of 12-molybdophosphoric acid hydrate (PMA, Alfa Aesar, M_w = 1825.25 g mol^{-1}, lot #M29C036) in nitromethane, acetonitrile or ethanol for 1 min and then thoroughly rinsed with pure solvent, to remove PMA residues.

The samples were then shipped to the Stanford Synchrotron Radiation Lightsource to conduct GIWAXS measurements. The measurement was performed at beamline 11-3 in a He-filled chamber with an X-ray wavelength of 0.9752 Å, and the sample-to-detector distance of 250 mm. The incident angle was 0.12°. The data processing was conducted using the Igor software (WaveMetrics, Inc.) with the Nika and WAXStools packages,[34,35] considering an out-of-plane sector of 0–20° and an in-plane sector of 70–90°. In this work, 0° is defined as the vertical direction to the substrate, 90° is the parallel direction to the substrate.

Solar cell fabrication

ITO-coated soda lime float glass sheets (Colorado Concept Coatings LLC) with a sheet resistance of 9–15 Ω sq^{-1} were cleaved into 1″ by 1″ pieces to become substrates for the solar cells. The ITO substrates were patterned with Kapton tape and etched by acid vapors (1 : 3 by volume, HNO_3 : HCl) for 5 min at 80 °C. The patterned substrates were then solvent cleaned in sequential ultrasonic baths of Liquinox detergent in distilled water, distilled water, acetone and 2-propanol, each lasting 40 min and at a temperature of 40 °C. All substrates were blown dry with N_2 after each bath.

Polyethylenimine, 80% ethoxylated (PEIE) (M_w 110 000, 306185-Aldrich) dissolved in H_2O at a concentration of 37 wt% had previously been purchased from Sigma-Aldrich, further diluted with 2-methoxyethanol to a concentration of 0.1 weight% and left stirring overnight at 500 rpm inside a transparent vial in air. The 0.1 weight% PEIE solution was then spun coated on the cleaned ITO substrates at 5000 rpm, 928 rpm s^{-1} for 1 min, and the wet layer was annealed immediately after on a hot plate at 100 °C for 10 min, in air. Coated substrates were then transferred into a N_2-filled glove box for further processing.

Highly regioregular poly(3-hexylthiophene-2,5-diyl) (P3HT, Rieke Metals Item #4002-E, lot #BS19-90) had previously been mixed with Indene-C60 bisadduct (ICBA, Nano-C, lot #ICBA62-X02) in a 1 : 1 weight ratio, and dissolved into a 40 mg ml^{-1} solution using 1,2-dichlorobenzene. The solution was magnetically stirred overnight at 500 rpm at 70 °C, inside a nitrogen-filled glovebox.

The P3HT:ICBA solution was filtered through a 0.2 μm-pore PTFE filter and spun coated onto each glass/ITO/PEIE substrate at 800 rpm, 10 000 rpm s^{-1} for 30 s, dispensing 200 μl per sample. The resulting wet films were then slowly dried in covered glass Petri dishes for 3 h. After this solvent annealing process, a portion of the P3HT:ICBA dry layer was wiped off from the slides using chlorobenzene in order to expose the underlying ITO electrode to allow contact.

The ITO/PEIE/P3HT:ICBA slides were then thermally annealed on a hot plate set to 150 °C for 10 min inside the glovebox, and allowed to cool down in covered glass Petri dishes for 30 min. The thickness of the active layer is 200 nm, as measured using a spectroscopic ellipsometer (J. A. Woollam Co.). The thermally annealed samples were then p-doped by dipping them into a 0.5 M solution of 12-molybdophosphoric acid hydrate (PMA, Alfa Aesar, M_w = 1825.25 g mol^{-1}, lot #M29C036) dissolved in acetonitrile for various times (1 min, 10 min, and 30 min). Immediately after soaking, each doped sample was thoroughly rinsed with pure solvent to remove PMA residues from its surface.

Samples were then transferred through an antechamber to an adjacent nitrogen-containing glovebox which is integrated with a Kurt J. Lesker Spectros thermal evaporator. The slides were mounted onto a sample holder and affixed to a shadow mask with openings defining 5 rectangular-with-rounded-corners-shaped electrodes for individual devices. The vacuum chamber was pumped down to a base pressure of 1×10^{-7} Torr. The thermal evaporator system was then used to deposit 150 nm of Ag (at a rate of 0.1–3.0 Å s^{-1}). The completed devices were transferred in a sealed container to another N_2-filled glove box to conduct the electrical characterization.

Solar cell characterization

Current density–voltage (J–V) characteristics were measured inside the N_2-filled glove box using a source meter (2400, Keithley

Instruments, Cleveland, OH) controlled by a LabVIEW program. To test the solar cell properties under illumination, an Oriel lamp with an air mass 1.5 filter and an intensity of 100 mW cm^{-2} was used as the light source. Each device was covered with an aperture that had a defined area of 0.04 cm^2, and tested in the dark and under illumination conditions.

The devices were tested after fabrication, covered using aluminum foil and left in air, at room temperature. Current density–voltage (*J*–*V*) characteristics were measured in the following 524 h by placing samples inside the N_2-filled glove box and connecting them to the source meter (2400, Keithley Instruments, Cleveland, OH) controlled by the LabVIEW program. To test the solar cell properties under illumination, an Oriel lamp with an air mass 1.5 filter and an intensity of 100 mW cm^{-2} was used as the light source. Every time the devices were going to be measured, two characteristics were recorded: one after immediate illumination and another after 10 min of light soaking. The data was used to calculated the power conversion efficiency at each measuring instance.

Conflicts of interest

The authors declare no conflict of interest.

Acknowledgements

This research was supported in part by the Center for Organic Photonics and Electronics at Georgia Tech, by the Department of the Navy, Office of Naval Research Award No. N00014-14-1-0580 and N00014-16-1-2520, through the MURI Center for Advanced Photovoltaics (CAOP), and by the Air Force Office of Scientific Research through Award No. FA9550-16-1-0168. Also, the use of the Stanford Synchrotron Radiation Lightsource, SLAC National Accelerator Laboratory is supported by the U.S. Department of Energy, Office of Science, Office of Basic Energy Sciences under Contract No. DE-AC02-76SF00515. We also acknowledge the support of CONICYT (Chilean National Commission for Scientific and Technological Research) through the Doctoral Fellowship program ''Becas Chile'', Grant No. 72150387 for F. A. L., as well as support from COLCIENCIAS (Colombian Administrative Department of Science, Technology and Innovation) through the program Fulbright-Colciencias for V. A. R.-T., and the support of the Ministry of Science and Technology of Taiwan, Overseas Project for Postdoctoral Research Abroad Program (PRAP) (105-2917-I-564-044). This work was performed in part at the Georgia Tech Institute for Electronics and Nanotechnology, a member of the National Nanotechnology Coordinated Infrastructure, which is supported by the National Science Foundation (Grant ECCS-1542174).

References

1 C.-K. Lu and H.-F. Meng, *Phys. Rev. B: Condens. Matter Mater. Phys.*, 2007, **75**(1–6), 235206.
2 G. Heimel, I. Salzmann, S. Duhm and N. Koch, *Chem. Mater.*, 2011, **23**, 359–377.
3 D. T. Duong, C. Wang, E. Antono, M. F. Toney and A. Salleo, *Org. Electron.*, 2013, **14**, 1330–1336.
4 B. Lussem, C. M. Keum, D. Kasemann, B. Naab, Z. Bao and K. Leo, *Chem. Rev.*, 2016, **116**, 13714–13751.
5 I. Salzmann, G. Heimel, M. Oehzelt, S. Winkler and N. Koch, *Acc. Chem. Res.*, 2016, **49**, 370–378.
6 I. E. Jacobs and A. J. Moule, *Adv. Mater.*, 2017, **29**(1–39), 1703063.
7 A. Dai, A. Wan, C. Magee, Y. Zhang, S. Barlow, S. R. Marder and A. Kahn, *Org. Electron.*, 2015, **23**, 151–157.
8 C. Wang, D. T. Duong, K. Vandewal, J. Rivnay and A. Salleo, *Phys. Rev. B: Condens. Matter Mater. Phys.*, 2015, **91**(1–7), 085205.
9 J. Li, C. W. Rochester, I. E. Jacobs, S. Friedrich, P. Stroeve, M. Riede and A. J. Moule, *ACS Appl. Mater. Interfaces*, 2015, **7**, 28420–28428.
10 B. M. K. Walzer, M. Pfeiffer and K. Leo, *Chem. Rev.*, 2007, **107**, 1233–1271.
11 K.-G. Lim, S. Ahn, Y.-H. Kim, Y. Qi and T.-W. Lee, *Energy Environ. Sci.*, 2016, **9**, 932–939.
12 H. Kim, J. Byun, S.-H. Bae, T. Ahmed, J.-X. Zhu, S.-J. Kwon, Y. Lee, S.-Y. Min, C. Wolf, H.-K. Seo, J.-H. Ahn and T.-W. Lee, *Adv. Energy Mater.*, 2016, **6**(1–8), 1600172.
13 W. Gao and A. Kahn, *J. Appl. Phys.*, 2003, **94**, 359–366.
14 C. K. Chan, W. Zhao, S. Barlow, S. Marder and A. Kahn, *Org. Electron.*, 2008, **9**, 575–581.
15 M. Kröger, S. Hamwi, J. Meyer, T. Riedl, W. Kowalsky and A. Kahn, *Org. Electron.*, 2009, **10**, 932–938.
16 Y. Qi, T. Sajoto, M. Kröger, A. M. Kandabarow, W. Park, S. Barlow, E.-G. Kim, L. Wielunski, L. C. Feldman, R. A. Bartynski, J.-L. Brédas, S. R. Marder and A. Kahn, *Chem. Mater.*, 2010, **22**, 524–531.
17 Y. Qi, S. K. Mohapatra, S. Bok Kim, S. Barlow, S. R. Marder and A. Kahn, *Appl. Phys. Lett.*, 2012, **100**(1–4), 083305.
18 S. Guo, S. B. Kim, S. K. Mohapatra, Y. Qi, T. Sajoto, A. Kahn, S. R. Marder and S. Barlow, *Adv. Mater.*, 2012, **24**, 699–703.
19 J. Fuzell, I. E. Jacobs, S. Ackling, T. F. Harrelson, D. M. Huang, D. Larsen and A. J. Moule, *J. Phys. Chem. Lett.*, 2016, **7**, 4297–4303.
20 J. Li, C. W. Rochester, I. E. Jacobs, E. W. Aasen, S. Friedrich, P. Stroeve and A. J. Moulé, *Org. Electron.*, 2016, **33**, 23–31.
21 I. E. Jacobs, E. W. Aasen, D. Nowak, J. Li, W. Morrison, J. D. Roehling, M. P. Augustine and A. J. Moule, *Adv. Mater.*, 2017, **29**(1–8), 1603221.
22 I. E. Jacobs, F. Wang, N. Hafezi, C. Medina-Plaza, T. F. Harrelson, J. Li, M. P. Augustine, M. Mascal and A. J. Moulé, *Chem. Mater.*, 2017, **29**, 832–841.
23 R. Po, A. Bernardi, A. Calabrese, C. Carbonera, G. Corso and A. Pellegrino, *Energy Environ. Sci.*, 2014, **7**, 925–943.
24 S. Zhang, L. Ye, H. Zhang and J. Hou, *Mater. Today*, 2016, **19**, 533–543.
25 H. Zhang, H. Yao, W. Zhao, L. Ye and J. Hou, *Adv. Energy Mater.*, 2016, **6**(1–6), 1502177.

26 N. Aizawa, C. Fuentes-Hernandez, V. A. Kolesov, T. M. Khan, J. Kido and B. Kippelen, *Chem. Commun.*, 2016, **52**, 3825–3827.

27 V. A. Kolesov, C. Fuentes-Hernandez, W. F. Chou, N. Aizawa, F. A. Larrain, M. Wang, A. Perrotta, S. Choi, S. Graham, G. C. Bazan, T. Q. Nguyen, S. R. Marder and B. Kippelen, *Nat. Mater.*, 2017, **16**, 474–480.

28 P. J. Brown, H. Sirringhaus, M. Harrison, M. Shkunov and R. H. Friend, *Phys. Rev. B: Condens. Matter Mater. Phys.*, 2001, **63**(1–11), 125204.

29 P. J. Brown, D. S. Thomas, A. Köhler, J. S. Wilson, J.-S. Kim, C. M. Ramsdale, H. Sirringhaus and R. H. Friend, *Phys. Rev. B: Condens. Matter Mater. Phys.*, 2003, **67**(1–16), 064203.

30 E. Verploegen, R. Mondal, C. J. Bettinger, S. Sok, M. F. Toney and Z. Bao, *Adv. Funct. Mater.*, 2010, **20**, 3519–3529.

31 C. M. Proctor and T.-Q. Nguyen, *Appl. Phys. Lett.*, 2015, **106**(1–4), 083301.

32 B. Kippelen and J.-L. Brédas, *Energy Environ. Sci.*, 2009, **2**, 251–261.

33 Y. Zhou, J. W. Shim, C. Fuentes-Hernandez, A. Sharma, K. A. Knauer, A. J. Giordano, S. R. Marder and B. Kippelen, *Phys. Chem. Chem. Phys.*, 2012, **14**, 12014–12021.

34 J. Ilavsky, *J. Appl. Crystallogr.*, 2012, **45**, 324–328.

35 S. D. Oosterhout, V. Savikhin, J. Zhang, Y. Zhang, M. A. Burgers, S. R. Marder, G. C. Bazan and M. F. Toney, *Chem. Mater.*, 2017, **29**, 3062–3069.